ASIAN JOURNAL
OF ORGANIC CHEMISTRY

www.asianjoc.org

Accepted Article

Title: Synthesis of fluoro- and cyano-aryl containing pyrene derivatives and their optical and electrochemical properties

Authors: Xiaojie Gong, Darren Heeran, Qiang Zhao, Chaoyue Zheng, Dmitry S. Yufit, Graham Sandford, and Deqing Gao

To be cited as: *Asian J. Org. Chem* 10.1002/ajoc.201900018

Link to VoR: http://dx.doi.org/10.1002/ajoc.201900018

A Journal of

ACES
Asian Chemical Editorial Society

A sister journal of **Chemistry – An Asian Journal** and **European Journal of Organic Chemistry**

WILEY-VCH

FULL PAPER WILEY-VCH

Synthesis of fluoro- and cyano-aryl containing pyrene derivatives and their optical and electrochemical properties

Xiaojie Gong, ‡ [a] Darren Heeran, ‡ [b] Qiang Zhao,‡[a] Chaoyue Zheng, ‡ [a] Dmitry S. Yufit,[b] Graham Sandford*[b] and Deqing Gao*[a]

[a] X. J. Gong, C. Y. Zheng, Professor D.Q. Gao [ORCID 0000-0002-9920-342]
Key Laboratory of Flexible Electronics & Institute of Advanced Materials, Jiangsu National synergistic Innovation Center for Advanced Materials, Nanjing Tech University
Nanjing, Jiangsu 211816, P.R. China.
E-mail: iamdqgao@njtech.edu.cn
[b] Dr D. Heeran, Professor G. Sandford [ORCID 0000-0012-3266-2039]
Department of Chemistry
Durham University
South Road, Durham, DH1 3LE, U.K.
E-mail: Graham.Sandford@Durham.ac.uk

Supporting information for this article is given via a link at the end of the document

Abstract: Mono- and 1,6-disubstituted pyrene derivatives bearing perfluorotoluene or perfluorobenzonitrile moieties were synthesized by nucleophilic substitution processes. The compounds were characterized by NMR, UV-vis, photoluminescence (PL), thermal gravimetric analysis (TGA), differential scanning calorimetry (DSC), cyclic voltametry (CV) and density functional theory (DFT) calculations. We found that derivatives substituted with perfluorobenzonitrile showed better thermal stability, stronger electron with-drawing ability and better fluorescence properties than the corresponding perfluorotoluyl-pyrene systems

Introduction

Among various polyaromatic hydrocarbon rings, the chemistry of pyrene derivatives has been extensively explored, due to their thermal stability and unique photophysical properties.[1] Pyrene derivatives have been widely adopted as probes for temperature,[2] pH [3] and metal ions.[4,5] They have been also designed to present the non-linear optical (NLO)[6] and two-photo absorption (TPA) properties.[1,7] In organic light-emitting diodes (OLED),[8] pyrene derivatives have been widely investigated as emission layers due to their interesting properties such as pure blue emission and high quantum fluorescence yield. In recent years, much progress has been made in the application of pyrene-based organic systems in organic thin-film transistor (OTFT) devices because of the strong tendency of purene to aggregate in the solid state. However, most pyrene-based semiconductor materials reported so far are p-type systems[9] whereas only a few n-type materials have been described[10] because it is extremely difficult to develop n-type pyrene-based semiconductor materials due to high-lying HOMOs which limit stability in air. An effective approach to reduce polyaromatic hydrocarbon HOMO energies is by attaching functional electron-withdrawing groups such as fluorine (-F),[11] perfluoroalkyl ($-C_nF_{2n+1}$)[12] and cyano group[13] onto π-conjugated systems. This approach can increase the electron affinity (EA) of polyaromatic molecules to deliver ambient temperature-stable and electron-accepting properties.

At the same time, the introduction of electron-withdrawing groups at suitable positions on a pyrene scaffold can result in enhanced intramolecular charge-transfer (ICT). In the last few decades, push-pull structures consisting of an electron-donating (D) and electron-withdrawing (A) structure have been extensively studied in materials chemisty.[14] D-A systems play an important role in photophysics because of their high fluorescent quantum yield due to effective radiative decay of intramolecular charge transfer (ICT) processes in the excited state. ICT systems have been used in detection[15] due to their obvious color change in different environments such as solvent polarity and pH. In the field of organic electronics, they may show bipolar charge-transporting properties which could be modulated by tuning molecular donor and acceptor units.

Since fluorine is the most electronegative element, perfluoroaryl and perfluoroalkyl groups have been widely used in organic electronics applications due to their strong electron-withdrawing ability.[16] The C-H…F interactions can play an important role in supramolecular organization and π-stacking which enhance charge carrier mobility.[16b] In this context, we report the synthesis and properties of pyrene derivatives bearing perfluorotoluene, perfluorobenzonitrile and benzonitrile electron-withdrawing groups. Such systems can be expected to show interesting high electron affinity, electron-conducting and solvatochromism properties.

Results and Discussion

Synthesis

Several pyrene derivatives bearing polyfluoroaryl substituents were synthesized by following the strategy shown in **Scheme 1**. Key starting material 1-bromopyrene was prepared by reaction of HBr with a peroxide initiator. After 15 h, GC-MS revealed that the reaction mixture contained 82% monobrominated compound and 16% dibrominated compound, which was sufficient for work-

up and purification. Column chromatography on silica gel using hexane as the eluent gave the desired monobrominated product in 35 % yield.

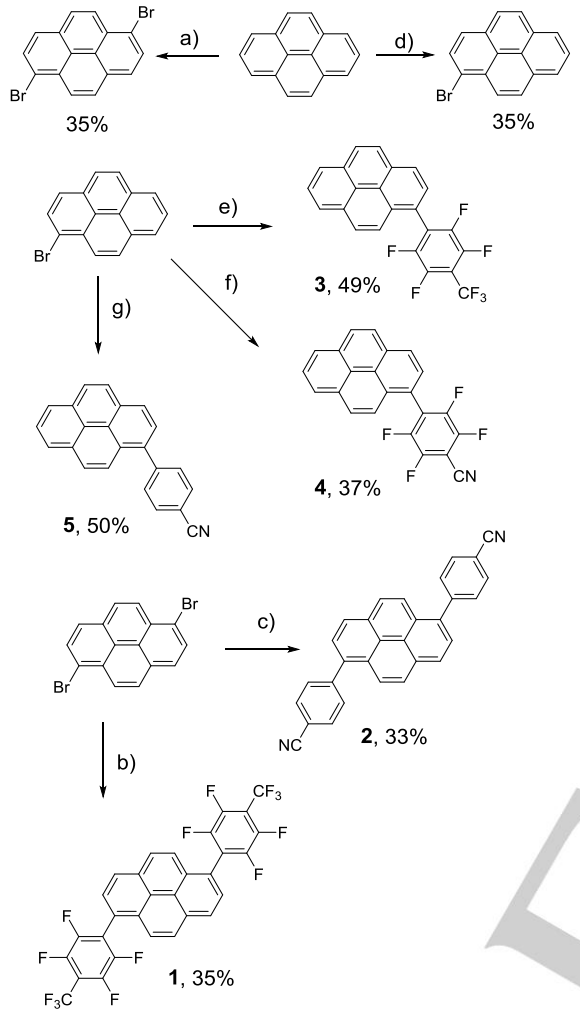

Scheme 1. Synthesis of pyrene derivatives: a) Br_2, CH_2Cl_2, r.t., 35%; b) *n*-BuLi, octafluorotoluene, THF, -78 °C, 35%; c) 4,4,5,5-tetramethyl-2-(4-cyanophenyl)-1,3,2-dioxaborolane, $Pd(PPh_3)_4$, Na_2CO_3, H_2O/toluene, 33%; d) HBr, H_2O_2, methanol, ether, r.t., 35%; e) *n*-BuLi, octafluorotoluene, THF, -78 °C, 49%; f) *n*-BuLi, pentafluorobenzonitirile, THF, -78 °C, 37%; g) 4,4,5,5-tetramethyl-2-(4-cyanophenyl)-1,3,2-dioxaborolane, $Pd(PPh_3)_4$, Na_2CO_3, H_2O/toluene, 50%.

Lithiation of 1-bromopyrene using *n*-BuLi to form the corresponding carbanion intermediate and subsequent reaction with octafluorotoluene gave **3** by an S_NAr process The carbanion was formed at -78 °C in THF and the addition of a large excess of octafluorotoluene limited possible side reactions. Subsequent recrystallization of the crude product mixture from hexane/dichloromethane yielded the desired product **3** in 49 % yield. The structure of **3** was confirmed by X-ray crystallography (Figure1a).

By a similar process, the reaction of pentafluorobenzene gave almost exclusively pyrene suggesting that proton abstraction from pentafluorobenzene is preferred to nucleophilic substitution at fluorine, due to the formation of a relatively stable perfluoroaryl anion. Hence, we decided to use a fluoraryl substrate, which does not possess an acidic proton, such as chloropentafluorobenzene. However, this substrate gave rise to a complex mixture with mass spectrometric analysis suggesting the formation of 1,6-dichloropyrene rather than the desired product via chlorophilic attack of the anion which is facilitated by the strong electron-withdrawing effect of the fluorine substituents. Reaction of pentafluorobenzonitrile with 1-bromopyrene by the S_NAr strategy gave the desired monoaryl product **4** in 37 % yield. Benzonitrile derivative **5** was synthesised by a palladium catalysed Suzuki-Miyaura coupling process.

Synthesis of 1,6-disubstituted pyrene analogues starting from 1,6-dibromopyrene were also carried out. Excess *n*-BuLi (3 eq.) was sufficient to form the corresponding lithiated species which readily reacted with a large excess of octafluorotoluene. The crude reaction mixture showed the major component to be the desired product alongside some residual starting material and small amounts of hydrodebrominated products. Initial purification attempts via recrystallization in various solvents proved difficult due to persistent contamination with reaction substrate leading to low isolated yields. The resulting crude product was purified by recrystallization from hexane/dichloromethane to give the diaryl pyrene product in 35% yield and the structure of **1** was confirmed by X-ray crystallography.

Molecule **1** in the crystal occupies a special position in the centre of symmetry (Figure 1a). The dihedral angles between planes of perfluorotoluyl substituents and pyrene planes in both **1** and **3** are similar, 62.1(2) and 58.9(2)° respectively. The crystal structures of non-fluorinated analogues of compounds **1** and **3** are not known but these values are in the usual range for Ph-substituted pyrenes.[17] In spite of the similarity of the molecules, the packing motifs in crystals **1** and **3** are quite different. No apparent π...π interactions are present in structure **1** and the pair-wise energy calculations[18] show almost isotropic distribution of the strongest intermolecular interactions in the structure of **1**. The main contribution into total energy is provided by dispersion forces. Molecules **3** in crystals form anti-parallel dimers augumented by short CH...F contacts and the distance between the pyrene planes is 3.44 Á. The π-π stacking is favorable for charge–carrier transport. However, the energy calculations show that the energy of interactions between molecules in such dimers (54.2 kJ/mol) is equal to that between the molecules, apprently connected by C-H...π contacts (54.6 kJ/mol) and thus the dimers cannot be regarded as the main "building block" of structure **3**. This is another example of the shortcomings of geometry-based analysis of intermolecular interactions.

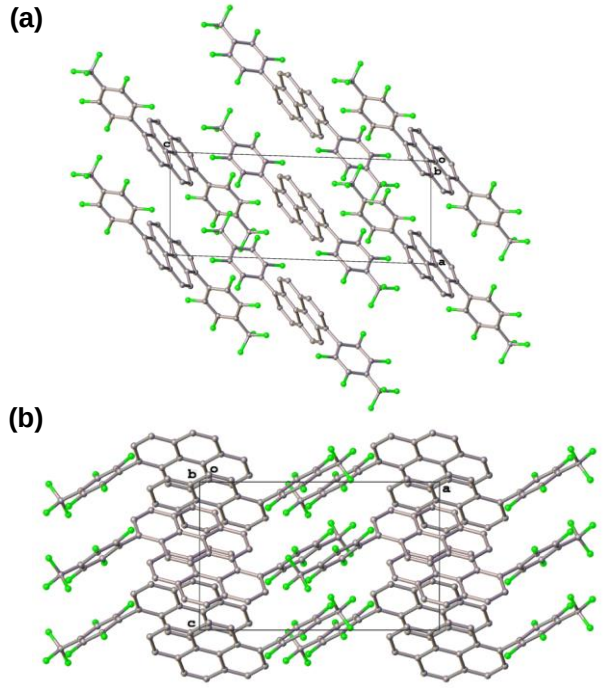

Figure 1. Molecular structures and packing of the single crystals of **3** (a) and **1** (b) determined by X-ray crystallography.

Optical and electrochemical properties

The UV-vis absorption spectra of pyrene derivatives were measured in dilute $CHCl_3$ solution at room temperature. Compared with the absorption characteristics of pyrene which is composed of two major absorption maxima at 274 nm and 336 nm with small vibronic bands at 260 nm, 307 nm and 321 nm,[19] all the pyrene derivatives in this work showed two red-shifted absorption ranges between 278-289 nm and 344-366 nm (Figure 2a). They are caused by the incorporation of the phenyl moieties which increased π conjugation in the structure, especially in the case of compound **2** with symmetrically disubstituted 4-cyanophenyl groups. Compounds **1**, **3** and **4** presented vibronic bands in the ranges of 266-274 nm and 313-338 nm. Around 380 nm, the fluoro-containing compounds **1**, **3** and **4** showed absorption shoulders, due to the presence of electron-withdrawing fluoroaryl rings which cause intramolecular charge transfer (ICT).

Compound **3** has one perfluorotoluene unit while compound **1** has two, so the absorption maximum of **1** at 353 nm was red-shifted by 9 nm relative to that of **3** at 344 nm. A similar phenomenon was observed in the case of compounds **5** and **2**, and the absorption maximum of **2** at 366 nm was red-shifted by 18 nm relative to that of **5** at 348 nm. Relative to **1**, the absorption of **2** was red-shifted by 13 nm perhaps due to the colour auxiliary effect of –CN and longer conjugate structure. This phenomenon was similar in the case of compounds **3** and **4**. The absorption spectrum of **4** at 344 nm became broader compared with that of **1** and **3**, and the intensity of a shoulder peak around 380 nm was higher than that of **1** and **3**, which means ICT processes occur more easily in compound **4** than in **1** and **3**. The absorption spectra of pyrene derivatives remained unaffected by solvent polarity, which indicated the interaction of these pyrene systems with solvents in the ground state were less significant.[20]

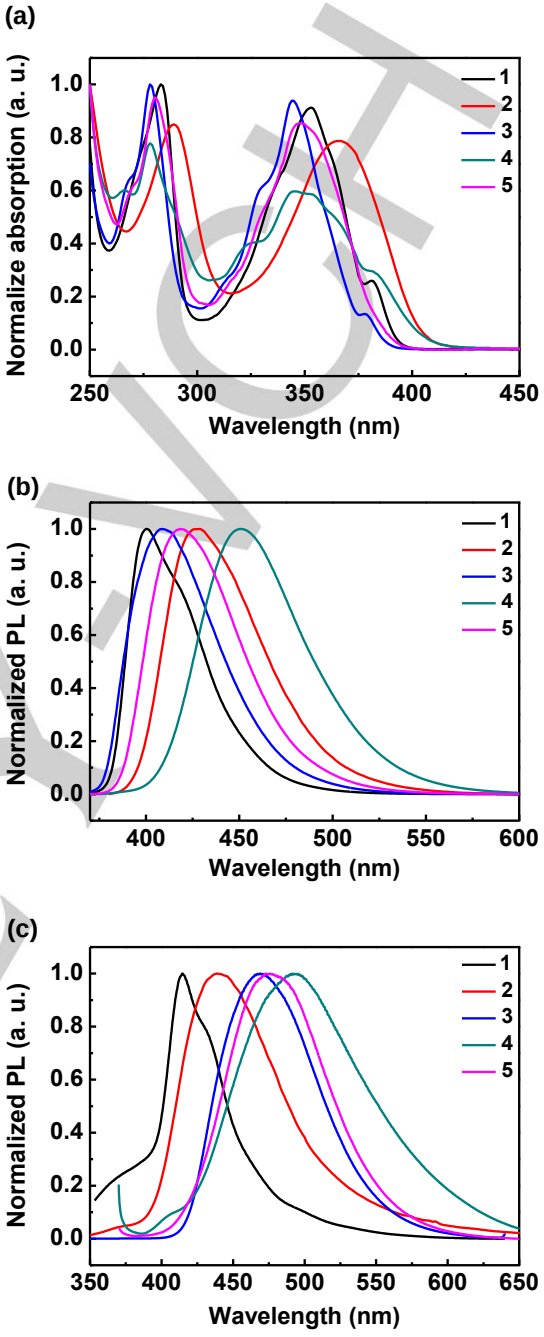

Figure 2. UV-vis absorption (a) in dilute $CHCl_3$ solution, and photoluminescence in dilute $CHCl_3$ solution (b) and in the film state (c) of pyrene derivatives.

The luminescence spectra of the pyrene derivatives in dilute solution were measured in chloroform at room temperature. Symmetrically disubstitued **2** with an emission maximum at 428 nm was red-shifted relative to **1** with a maximum at 400 nm due to cyano-containing phenyl groups largely extending conjugation (seen in Figure 2b). The same observation is seen for mono-substituted derivatives, **4** with a maximum of 452 nm and **3** with

a maximum of 409 nm. Whether the ICT effect is attributed to the fluorine substituent or the extension of the conjugation over a cyano group or aryl substituents depends on the chemical struture. In the fluoro-compounds **1** and **3**, ICT was dominant and mono-substituted **3** was red-shifted. **5**, with a maximum at 419 nm, has a benzonitrile moiety and **4** has tetrafluorobenzonitrile moieties. ICT was dominant as well and **4** was red-shifted. In the cyano-compounds of **2** and **5**, conjugation extension was dominant and disubstituted **2** was red-shifted.

Compared with the emission in solution, compounds **1** and **2** showed unobvious red-shifted phenomenon in the film state due to loose stacking in the solid state (Figure 2c), as observed in 1,6-disubstituted pyrene derivatives.[21]

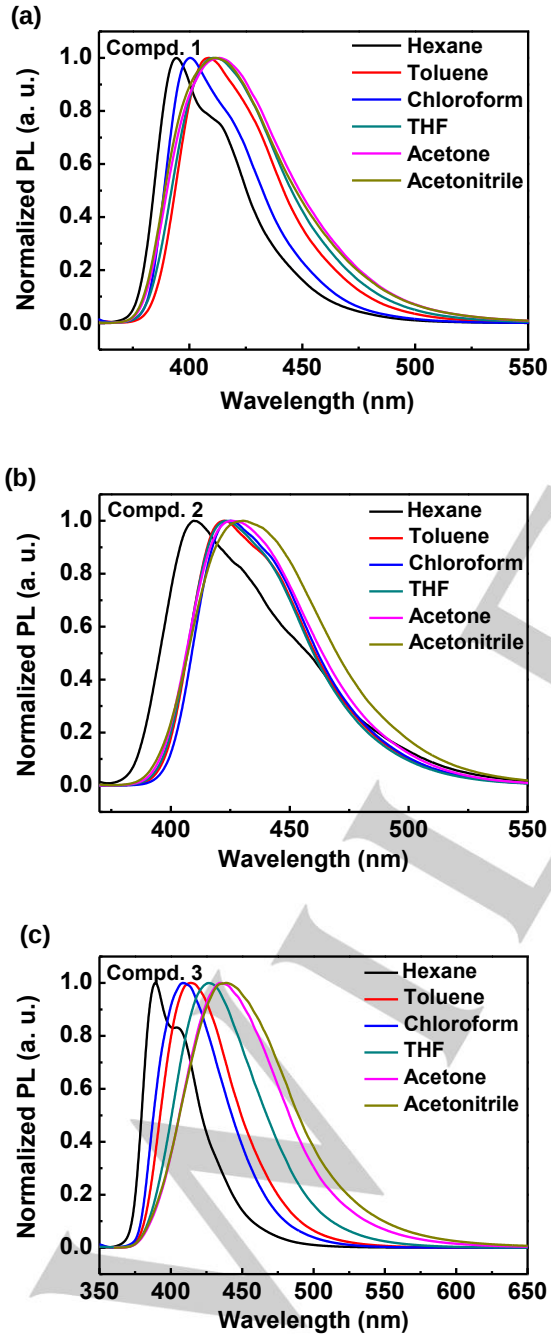

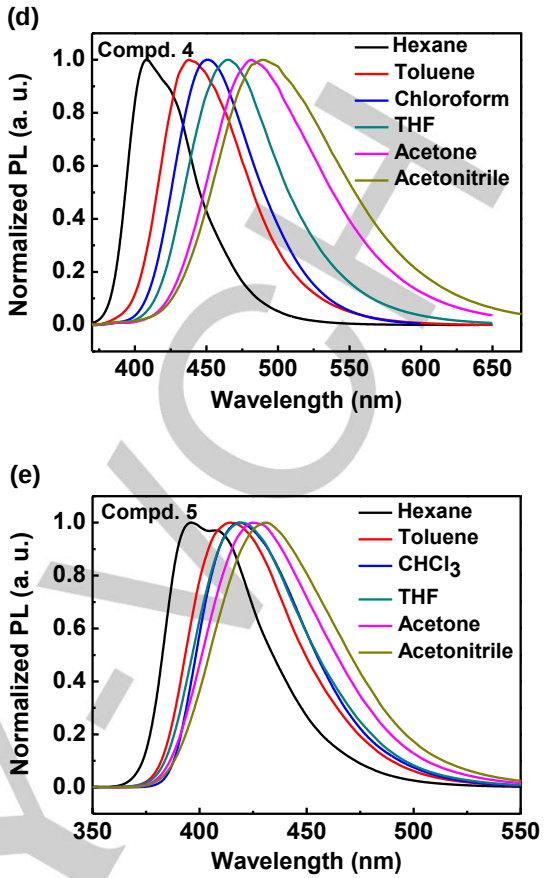

Figure 3. Solvatochromism of pyrene derivatives in solution: (a) compound **1;** (b) compound **2;** (c) compound **3;** (d) compound **4;** (e) compound **5.**

Table 1. Solvatochromism of pyrene derivatives.

	Hexane[a]	Toluene	$CHCl_3$	THF	Acetone	Acetonitrile
1	395 (413)	408	400	410	413	411
2	410 (430)	421	425	422	425	431
3	388 (405)	415	408	426	435	439
4	407	438	452	465	481	490
5	398 (409)	415	419	419	426	432

[a] Shoulder peaks in bracket.

Intramolecular charge-transfer (ICT) chromophores with an electron acceptor and an electron donor often possess useful solvatochromatic properties. In nonpolar solvents, the chromophores form local excited (LE) states which contribute to high fluorescent efficiency whereas, in highly polar solvents, fluorescent spectra reveal a remarkable red-shift due to the formation of an intramolecular charge-transfer (ICT) excited state.[22] In our systems, pyrene acts as the electron-donating moiety and the phenyl bearing electron-withdrawing groups acts as corresponding electron-accepting moiety, thus the systems is expected to show ICT properties. The solvatochromism properties of pyrene derivatives were studied by measuring the

fluorescence spectra in a series of nonpolar to polar solvents. As in Figure 3, mono-substituted compounds **3**, **4** and **5** had stronger solvatochromism than di-substituted compounds **1** and **2**, especially compound **4** which displayed the redshift of 83 nm on going from hexane to acetonitrile solution and the spectrum became broader (Figure 3d). It indicates that the excited states of compound **4** have a large polarity which originates from the formation of an excited-state intramolecular charge transfer (ICT) where the electronic structure of the compound is rearranged in response to environmental polarity, as commonly observed in electron donor-π-acceptor (D-π-A) systems. Compound **1** (Figure 3a) and **2** (Figure 3b) gave red shifts of 20 nm from nonpolar hexane to highly polar acetonitrile solution, being attributed to their small dipole moments in the symmetrical structures.[23] For all pyrene-based derivatives, spectroscopic vibronic structure appeared in hexane but disappeared in more polar solvents. The disappearance of the vibronic structure in polar solvents indicates that ICT from the pyrene moiety to the electron-withdrawing moiety is enhanced when polar solvents are used and strong electronic interaction between the perfluorophenyl and pyrene moieties results in these unstructured fluorescence bands.

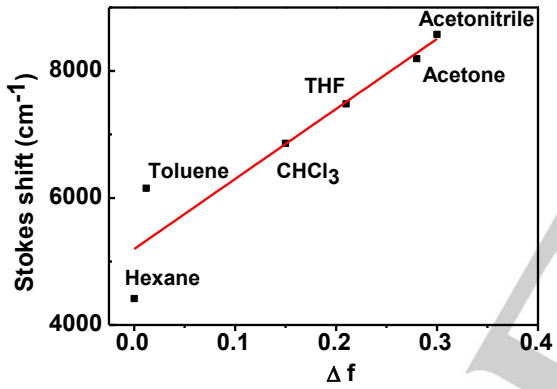

Figure 4. Fluorescence Stokes shifts as a function of orientational polarizability Δ*f* in various solvents for **4.**

To better evaluate the effect of solvent on the emission features of **4** which showed the strongest solvatochromism, the relationship between the solvent polarity parameter (Δf) and the Stokes shift ($\Delta \nu$) was investigated using the Lippert–Mataga equation:

$$\Delta \nu = \frac{1}{4\pi\varepsilon_o hca^3}\frac{2\Delta m\mu^2}{hcR^3}\Delta f + \text{const.}$$

where $\Delta \nu$ is the Stokes shift, Δm_μ is the difference of the dipole moment of solute molecule between excited (μ_e) and ground states (μ_g), *h* is Planck's constant, R is the radius of the solvent cavity in which the chromophore resides (Onsager cavity radius), and Δ*f* is the orientation polarizability of the solvent. As observed in Figure 4, the linear relationship of Stokes shift against the solvent's polarizability was obtained and the energy of the singlet excited states was decreased with the increase of the polarity of the solvents.[24] The other derivatives was treated in the same way but no linearity of fluorescence Stokes shifts was observed because of their weaker ICT effect.

Electrochemical behaviour

The electrochemical behavior of the pyrene derivatives was investigated by cyclic voltammetry (CV) in a standard three-electrode electrochemical cell using 0.1 M tetrabutylammonium hexafluorophosphate in dry chloroform solutions at room temperature under nitrogen with a scanning rate of 50 mV/s. A glassy carbon working electrode, a platinum counter electrode and an Ag/AgCl (0.1 M) reference electrode were utilized. The measurements of the derivatives displayed one oxidation process in chloroform solution, but no obvious reduction peaks were detected (seen in Figure 5). The oxidation onset potentials were measured to be 1.45, 1.29, 1.34, 1.41 and 1.12 V, respectively. Therefore, the corresponding HOMO energy levels [HOMO = –(4.4 + E_{onset})] were estimated to be -5.85, -5.69, -5.74, -5.81 and -5.52 eV for **1, 2, 3, 4** and **5**, respectively. The optical band gaps (E_g^{opt}) obtained from the absorption edges were 3.16, 3.06, 3.19, 3.05 and 3.16 eV for **1, 2, 3, 4** and **5**, respectively. By using the formula: HOMO = LUMO − E_g^{opt}, the LUMO energy levels were -2.69, -2.63, -2.55, -2.76 and -2.36 eV, respectively. The physical properties of the pyrene derivatives are summarized in Table 2.

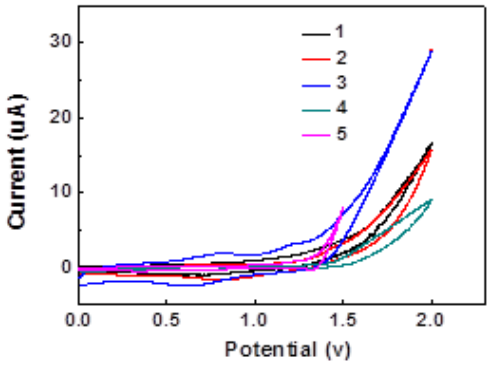

Figure 5. Electrochemical behaviors of the pyrene derivatives.

Table 2. Summary of the physical properties of pyrene derivatives.

	Abs[a] (nm)	PL (nm)		HOMO (eV)		LUMO (eV)		T_d[f] (°C)
		Sol[b]	Film[c]	CV[d]	DFT[e]	CV[d]	DFT[e]	
1	283, 352, 381	400	414	-5.85	-5.96	-2.69	-2.40	300
2	288, 367	428	440	-5.69	-5.69	-2.63	-2.28	192
3	278, 344	409	470	-5.74	-5.65	-2.55	-2.02	262
4	265, 278, 321, 345, 384	452	495	-5.81	-5.74	-2.76	-2.30	412
5	280, 345	419	478	-5.52	-5.53	-2.36	-1.96	329

[a,b] Measured in the diluted $CHCl_3$ solution at room temperature.

[c] Films at a quartz substrate.

[d] Determined by cyclic voltammetry.

[e] From Density functional theory (DFT) calculations.

[f] Decomposition temperature corresponding to 5% weight loss measured by TGA.

Theoretical Investigations

To obtain a better insight into the relationship between structure and property at the molecular level, density functional theory (DFT) calculations using the Gaussian 03 program at the B3LYP/6-31G(d) level were carried out to evaluate the positions and energies of frontier orbitals for the pyrene derivatives. For all derivatives, the electron-withdrawing group-containing phenyl substituent mainly contributes to the distribution of the LUMO orbital while almost all the HOMO orbital is positioned on the pyrene moiety, meaning that a charge-transfer process could occur from pyrene moiety to the electron-withdrawing group-containing phenyl moiety. The dihedral angel between phenyl and pyrene moieties is about 60° for all the derivatives (seen in Figure 7), corresponding well to the experimental values found in crystal structures of **1** and **3**.

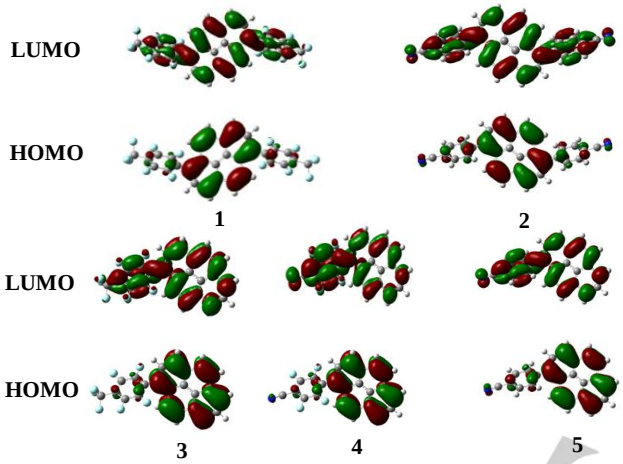

Figure 6. Computed molecular orbital plots of pyrene derivatives.

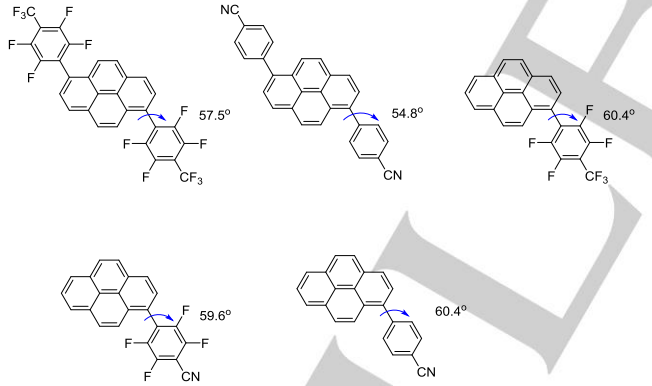

Figure 7. Computed dihedral angel between pyrenyl and phenyl planes for the derivatives.

Thermal properties

The thermal properties of the fluorescent materials were determined by thermogravimetric analysis (TGA) and differential scanning calorimetry (DSC) measurements. As shown in Figure 8 the onset decomposition temperatures (T_d) (the temperature corresponding to 5% weight loss) of pyrene derivatives were estimated to be 300 °C for **1**, 192 °C for **2**, 262 °C for **3**, 412 °C for **4** and 329 °C for **5**. They had high thermal stability, partially attributed the *para*-position of the phenyl which affects the thermal properties.[24] In DSC measurement (Figure 9), melting temperature (215°C) and crystallization temperature (126°C) was observed for compound **3** but no phase transition was observed in the DSC scan for other compounds.

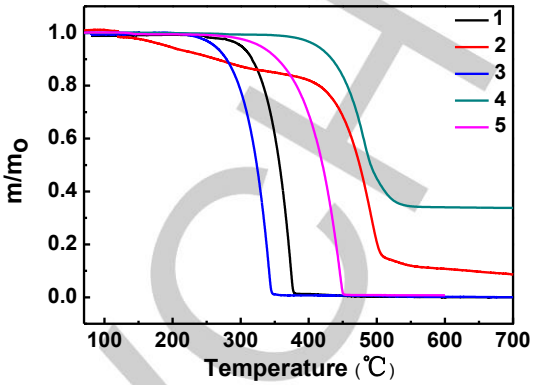

Figure 8. TGA analysis of pyrene derivatives.

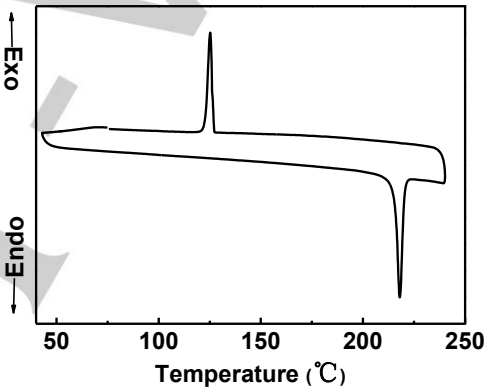

Figure 9. DSC curve for compound **3**.

Conclusions

In summary, we have reported five pyrene-based materials bearing mono- and di-substituted perfluorotoluene, perfluorobenzonitrile and benzonitrile moieties as promising candidates for n-type semiconductors. The polyfluorinated compounds were synthesized by S_NAr type processes. The single crystals of the materials with mono- and di-substituted perfluorotoluene susbstituents were analysed. The mono-aryl compound has close stacking and forms anti-parallel dimers due to short CH...F contact and the distance between pyrene planes was 3.44 Á. The thermal, optical, electrochemical and solvatochromism properties of the pyrene systems were investigated. The solvatochromism study interestingly reflected the PL dependence of the five compounds on the number and structure of the aryl substituent on going from nonpolar to polar solvent. The cyano groups contribute by extending π conjugation systems while fluorine substituents induce intramolecular charge transfer. The mono-aryl compounds had stronger solvatochromism than di-aryl compounds and fluoroaryl-pyrenes had stronger solvatochromism than nonfluoroaryl-compounds, which is attributed to the synergy of conjugation and intramolecular charge transfer.

Experimental Section

Materials

Pyrene, n-butyllithium (2.5 M in hexane) (n-BuLi), 4-iodobenzonitrile, octafluorotoluene, pentafluorobenzonitirile, methyl trioctyl ammonium chloride and tetrakis(triphenylphosphine) palladium(0) [$Pd(PPh_3)_4$] were purchased from Energy Chemical or Sigma-Aldrich. Bromine, hydrobromic acid (48 wt% aq), hydrogen peroxide (30 wt% aq) and sodium carbonate were purchased from Sinopharm and used without any further purification. Anhydrous THF was distilled over sodium-benzophenone system in nitrogen before use. Anhydrous $CHCl_3$ was distilled over CaH_2 before use.

General

NMR spectra were recorded on either a Bruker AMX 300 (^{1}H NMR, 300 MHz; ^{13}C NMR, 75 MHz) or a Bruker 400 Ultrashield (^{1}H NMR, 400 MHz; ^{13}C NMR, 101 MHz; ^{19}F NMR, 376 MHz) spectrometer in $CDCl_3$. UV-vis spectra were recorded on Shimadzu UV-1750. Infra-red (IR) spectra were recorded on a Perkin Elmer FTIR Spectrum TwoTM fitted with an ATR probe. Accurate mass analysis was achieved with a QtoF Premier mass spectrometer (Waters Ltd, UK) or an LCT Premier XE mass spectrometer (Waters Ltd, UK) equipped with an accurate solids analysis probe (ASAP).Fluorescence spectra were recorded on Hitachi F-4600. Cyclic voltammetry (CV) experiments were performed with a CHI-621B electrochemical analyzer. All measurements were carried out at room temperature with a conventional three electrode configuration consisting of a platinum counter electrode, a glassy carbon working electrode and a non-aqueous Ag/AgCl reference electrode. The solvent was degassed dry $CHCl_3$ in CV measurement. The supporting electrolyte was tetrabutylammonium hexafluorophosphate (n-Bu_4NPF_6). Thermaogravimetric analysis (TGA) was performed on a Perkin Elmer TGA7 thermal analyzer at a heating rate of 10 °C/min under dry N_2 flow. Differential scanning calorimetry (DSC) measurement was performed on NETZSCH DSC214 Polyma instrument under a heating rate of 10 °C/min and a nitrogen flow rate of 20 cm^3/min.

All NMR spectra are available in the Supporting Information.

Synthesis

1-Bromopyrene: To a methanol/ether (1:1) solution of pyrene (2.02 g, 10mmol) and hydrobromic acid (1.25 mL, 48 wt% aq., 11 mmol) was slowly added hydrogen peroxide (1.05 mL, 30 wt% aq., 10 mmol) over a period of 15 min and the reaction mixture was stirred at rt for 15 h. The solvent was removed and the product partitioned between dichloromethane (100 mL) and water (100 mL). The aqueous layer was extracted with dichloromethane (2 x 50 mL) and the combined organic extracts were washed with saturated sodium bicarbonate solution (2 x 100 mL) and saturated brine solution (100 mL) before being dried ($MgSO_4$) and concentrated. The crude product was purified by column chromatography on silica gel using hexane as the eluent to yield 1-bromopyrene (0.97 g, 35 %) as a white solid. ^{1}H NMR (400 MHz, $CDCl_3$): 8.40 (d, 1H, J = 9.2 Hz), 8.21–8.18 (m, 3H), 8.12 (d, 1H, J = 9.3 Hz), 8.06–7.95 (m, 4H). ^{13}C NMR (101 MHz, $CDCl_3$): 131.2, 131.0, 130.7, 130.1, 129.7, 129.0, 127.8, 127.2, 126.6, 126.0, 125.9, 125.8, 125.6, 125.6, 120.0. HRMS (ASAP) for $[M]^+$ $C_{16}H_9Br$ m/z: calculated 279.9888; found 279.9875. FT-IR (neat, cm^{-1}): 3034, 1600, 1589, 1428, 1015.

1,6-Dibromopyrene: 1,6-Dibromopyrene was prepared according to our previous reports.[25] A solution of bromine (2.0 ml) in dichloromethane (50 ml) was added dropwise to a solution of pyrene (4.0 g) in dichloromethane (70 ml) at room temperature over 2 hours. The reaction mixture was then stirred overnight at room temperature. The white precipitate was collected by filtration. 1,6-Dibromopyrene was obtained by recrystallization from toluene for several times as needle like crystals with the yield of 35%. ^{1}H NMR ($CDCl_3$, 300 MHz) δ: 8.48 (d, 2H, J = 9 Hz), 8.27 (d, 2H, J = 9 Hz), 8.12 (d, 2H, J = 9 Hz), 8.06 (d, 2H, J = 9 Hz).

4,4,5,5-tetramethyl-2-(4-cyanophenyl)-1,3,2-dioxaborolane: The mixture of 4-bromobenzenecarbonitrile (1.82 g, 10 mmol), potassium acetate (2.34 g, 30 mmol), bis(pinacontato) diboron (2.80 g, 11 mmol), $Pd(dppf)Cl_2$ (0.036 g, 0.030 mmol) in DMSO (25 ml) was heated under a nitrogen atmosphere at 80 ℃ overnight. The reaction mixture was cooled to room temperature, then cool water was added. The solution was extracted by ethyl acetate and the combined organic phase was dried over anhydrous $MgSO_4$. After the solvent was evaporated, column chromatography (silica gel, ethyl acetate/petroleum ether = 1/8, *v/v*) gave 4,4,5,5-tetramethyl-2-(4-cyanophenyl)-1,3,2-dioxaborolane (1.50 g, 75 %) as a white solid. ^{1}H NMR ($CDCl_3$, 300 MHz): 7.88 (d, 2H), 7.64 (d, 2H), 1.35 (s, 12H).

1,6-Di[2,3,5,6-tetrafluoro-4-(trifluoromethyl)phenyl]pyrene (1): A suspension of 1,6-dibromopyrene (0.72 g, 2 mmol) in dry THF (30 mL) was cooled to -78 ºC under an argon atmosphere. n-BuLi (2.4 mL, 2.5 M in hexane, 6 mmol) was added dropwise over 15 min and stirred at -78 °C for 2 h. Octafluorotoluene (2.08 g, 8.8 mmol) was added and the solution stirred overnight at rt before quenching with water (100 mL) and extraction with dichloromethane (3 x 100 mL). The combined organic extracts were washed with water (100 mL) and saturated brine solution (100 mL) before being dried ($MgSO_4$) and concentrated. The crude product was purified by column chromatography on silica gel using a gradient of hexane/ dichloromethane as the eluent followed by recrystallization from hexane/dichloromethane to yield 1,6-di[2,3,5,6-tetrafluoro-4-(trifluoromethyl)pheny]pyrene (0.44 g, 35 %) as off-white solid; Mp: 305-308 °C. ^{1}H NMR (400 MHz, CD_2Cl_2): 8.42 (d, 2H, $^3J_{HH}$= 7.9 Hz), 8.26 (d, 2H, $^3J_{HH}$ = 9.2 Hz), 8.06 (d, 2H, $^3J_{HH}$ = 7.9 Hz), 7.88 (dt, 2H, $^3J_{HH}$ = 9.2 Hz, $^5J_{HF}$ = 2.0 Hz).^{19}F NMR (376 MHz, CD_2Cl_2): -56.56 (t, 6F, $^4J_{FF}$ = 21.7 Hz), -138.13 – -138.28 (m, 4F), -140.78 – -141.11 (m, 4F). HRMS (ASAP) calculated for $[M]^+$ $C_{30}H_8F_{14}$ m/z: 634.0402; found 634.0413. FT- IR (neat, cm^{-1}): 1661, 1476, 1334, 1125, 984, 850, 713. *Crystal data*: $C_{30}H_8F_{14}$, M = 634.36, monoclinic, space group P $2_1/n$, a = 7.0080(1), b = 9.3436(1), c = 17.7678(3) Å, β = 92.01(1)°, U = 1162.72(3) Å^3, F(000) = 628, Z = 2, D_c = 1.812 mg m^{-3}, μ = 0.184 mm^{-1} (Mo-Kα, λ = 0.71073 Å), T = 120(1)K. 24921 collected reflections yielded 3388 unique data (R_{merg} = 0.0337). Final $wR_2(F^2)$ = 0.1084 for all data (199 refined parameters), conventional $R_1(F)$ = 0.0392 for 2784 reflections with I ≥ 2σ, GOF = 1.019. CCDC-1871282.

1,6-Di(4-benzonitrile)pyrene (2): A mixture of 1,6-dibromopyrene (0.36 g, 1 mmol), 4,4,5,5-tetramethyl-2-(4-cyanophenyl)-1,3,2-dioxaborolane (0.6 g, 3 mmol), methyl trioctyl ammonium chloride, toluene (25 mL) and 2 M Na_2CO_3 aqueous solution (5 mL) was bubbled with nitrogen for 20 minutes. Then $Pd(PPh_3)_4$ (46 mg, 0.04 mmol) was added to the mixture. The mixture was heated at 100 °C for 24 h under the atmosphere of nitrogen before being cooled to r.t. and extracted with dichloromethane (3 x 80 mL). The combined organic extracts were washed with water (100 mL) and saturated brine solution (100 mL) before being dried ($MgSO_4$) and concentrated. The crude product was purified by column chromatography on silica gel using dichloromethane and petroleum ether (1/1, *v/v*) as the eluent to yield 1,6-di(4-benzonitrile)pyrene (100 mg, 33%) as greenish yellow solid. ^{1}H NMR ($CDCl_3$, 300 MHz): 8.26 (d, 2H, J = 9.0 Hz), 8.11 (s, 4H), 7.98 (d, 2H, J = 6.0 Hz), 7.88 (d, 4H, J = 6.0 Hz), 7.77 (d, 4H, J = 6.0 Hz). ^{13}C NMR was not obtained due to low solubility in $CDCl_3$. MS (MALDI-TOF) *m/z*: calcd. for $C_{30}H_{16}N_2$, 404.47; found 404.97 (M^+).

1-[2,3,5,6-Tetrafluoro-4-(trifluoromethyl)phenyl]pyrene (3): A solution of 1-bromopyrene (0.42 g, 1.5 mmol) in dry THF (15 mL) was cooled to -78 ºC under an argon atmosphere. n-BuLi (0.88 mL, 2.5 M in hexane, 2.2 mmol) was added dropwise over 15 min and the solution was stirred at -78 ºC for 2 h. Octafluorotoluene (0.89 g, 3.75 mmol) was added and the reaction mixture was stirred overnight at rt before quenching with water

(50 mL) and extracted with dichloromethane. The combined organic extracts were washed with water (100 mL) and saturated brine solution (100 mL) before being dried ($MgSO_4$) and concentrated. The crude product was recrystallized from hexane/dichloromethane to yield 1-[2,3,5,6-tetrafluoro-4-(trifluoromethyl)phenyl]pyrene (0.31 g, 49 %) as a light green solid. Mp: 214-216 ºC. ^{1}H NMR (400 MHz, $CDCl_3$): 8.30 – 8.06 (m, 7H), 7.94 (d, 1H, J_{HH} = 7.9 Hz), 7.73 (1H, dt, $^3J_{HH}$ = 9.2 Hz, $^5J_{HF}$ = 2.1 Hz). ^{19}F NMR (376 MHz, $CDCl_3$): -56.09 (3F, t, $^4J_{FF}$ = 21.7 Hz), -137.35 – -137.56 (m, 2F), -140.09 – -140.47 (m, 2F). HRMS (ASAP) calculated for $[M]^+$ $C_{23}H_9F_7$ m/z: 418.0589; found 418.0592. FT-IR (neat, cm^{-1}): 1656, 1596, 1476, 1338, 1252, 1146. *Crystal data*: $C_{23}H_9F_7$, M = 418.30, monoclinic, space group P 2_1/c, a = 13.9115(6), b = 13.8263(6), c = 8.5615(4) Å, β = 90.10(1)°, U = 1646.8(1) Å^3, F(000) = 840.0, Z = 4, D_c = 1.687 mg m^{-3}, μ = 0.153 mm^{-1} (Mo-Kα, λ = 0.71073 Å), T = 120(1)K. 26934 collected reflections yielded 4785 unique data (R_{merg} = 0.0412). Final $wR_2(F^2)$ = 0.1177 for all data (307 refined parameters), conventional $R_1(F)$ = 0.0434 for 3538 reflections with I ≥ 2σ, GOF = 1.028. CCDC-1871283.

1-(2,3,5,6-Tetrafluorobenzonitrile)pyrene (4): A solution of 1-bromopyrene (0.84 g, 3 mmol) in dry THF (30 mL) was cooled to -78 ºC under an argon atmosphere. n-BuLi (1.76 mL, 2.5 M in hexane, 4.4 mmol) was added dropwise over 15 min and the solution stirred at -78 °C for 2 h. Pentafluorobenzonitrile (1.45 g, 7.5 mmol) was added and stirred overnight at rt before quenching with water (100 mL) and extracted with dichloromethane (3 x 50 mL). The combined organic extracts were washed with water (100 mL) and saturated brine solution (100 mL) before being dried ($MgSO_4$) and concentrated. The crude product was recrystallized from hexane/dichloromethane to yield 1-(2,3,5,6-tetrafluorobenzonitrile)pyrene (0.42 g, 37 %) as a yellow solid; Mp: 204-207 ºC. ^{1}H NMR (400 MHz, $CDCl_3$): 8.31–8.07 (m, 7H), 7.92 (d, 1H, $^3J_{HH}$ = 7.9 Hz), 7.69 (dt, 1H, $^3J_{HH}$ = 9.2 Hz, $^5J_{HF}$ = 2.1 Hz). ^{19}F NMR (376 MHz, $CDCl_3$): -132.00 – -132.15 (m, 2F), -135.88 – -136.03 (m, 2F). HRMS (ASAP) m/z calculated for $[M]^+$ $C_{23}H_9F_4N$375.0671; found 375.0662. FT-IR (neat, cm^{-1}): 3045, 2245, 1652, 1481, 1308, 979, 847.

1-(4-Benzonitrile)pyrene (5): A solution of 1-bromopyrene (0.281 g, 1 mmol), 4,4,5,5-tetramethyl-2-(4-cyanophenyl)-1,3,2-dioxaborolane (0.3 g, 1.5 mmol), methyl trioctyl ammonium chloride, toluene (25 mL) and 2 M Na_2CO_3 aqueous solution (5 mL) was purged with nitrogen for 20 minutes. $Pd(PPh_3)_4$ (46 mg, 0.04 mmol) was added to the mixture which was then heated at 100 °C for 24 h under the atmosphere of nitrogen before being cooled to r.t. and extracted with dichloromethane (3 x 80 mL). The combined organic extracts were washed with water (100 mL) and saturated brine solution (100 mL) before being dried ($MgSO_4$) and concentrated. The crude product was purified by column chromatography on silica gel using petroleum ether and dichloromethane (2/1, *v/v*) as the eluent to yield 1-(4-benzonitrile)pyrene (0.46 g, 50 %) as a light green solid. ^{1}H NMR ($CDCl_3$, 300 MHz): 8.26 – 8.02 (m, 8H), 7.93 (d, 1H, *J* = 6.0 Hz), 7.85 (d, 2H, *J* = 9.0 Hz), 7.75 (d, 2H, *J* = 9.0 Hz). ^{1}H NMR spectra was in accord with the literature.[26]

X-Ray crystallography. The X-ray single crystal data have been collected using λMoKα radiation (λ = 0.71073 Å) on a Bruker D8Venture (Photon100 CMOS detector, IμS-microsource, focusing mirrors) diffractometer equipped with a Cryostream (Oxford Cryosystems) open-flow nitrogen cryostat at the temperature 120.0(2) K. All structures were solved by direct method and refined by full-matrix least squares on F^2 for all data using Olex2 software[27] and SHELXTL software[28]. Crystallographic data for the structure have been deposited with the Cambridge Crystallographic Data Centre as supplementary publications CCDC-1871282, 1871283.

Acknowledgements

‡The first four authors contributed equally to this work. We thank the International Exchange Program under grant No. 21511130059 between the National Natural Science Foundation of China and the Royal Society of United Kingdom of Great Britain.

Keywords: pyrene • fluorine atom • Intramolecular charge transfer • n-type semiconductor

References:

1. H. M. Kim, Y. O. Lee, C. S. Lim, J. S. Kim and B. R. Cho, *J. Org. Chem.,* 2008, **73**, 5127-5130.
2. Q. -Y. Fang, J. -W. Li, S. -Y. Li, R. -H. Duan, S. -Q. Wang, Y. -P. Yi, X. -D, Guo, Y. Qian, W. Huang and G. -Q. Yang, *Chem. Commun.,* 2017, **53**, 5702-5705.
3. (a) J. -B. Chao, H. -J. Wang, Y. -B. Zhang, C. -X. Yin, F. -J. Huo, K. -L. Song, Z. -Q. Li, T. Li and Y. -Q. Zhao, *Talanta.,* 2017, **174**, 468-476. (b) B. -B. Ma, G. -F. Feng, P. -C. Zhao, F. -F. Chang and W. Huang, *Tetrahedron Lett.,* 2015, **56**, 6912-6914.
4. (a) C. Wu, Y. Ikejiri, J. -L. Zhao, X. -K. Jiang, X. -L. Ni, X. Zeng, C. Redshaw and T. Yamato, *Sensors and Actuators B.,* 2016, **228**, 480-485. (b) Z. M. Sahin, D. Alimli, M. M. Tonta, M. E. Kose and F. Ylimaz, *Sensors and Actuators B.,* 2017, **242**, 362-368.
5. (a) M. Boonsri, K. Vongnam, S. Namuangruk, M. Sukwattanasintt and P. Rashatasakhon, *Sensors and Actuators B.,* 2017, **248**, 665-672. (b) A. Kumar, A. Pandith and H. -S. Kim, *Sensors and Actuators B.,* 2016, **231**, 293-301.
6. (a) Y. -F. Shi, Z. -G. Li, Y. Fang, J. -Y. Sun, M. -G. Zhao and Y. -L. Zhao, *Optics & Laser Technology.,* 2017, **90**, 18-21. (b) Z. -G. Xiao, Y. -F. Shi, R. Sun, J. -F. Ge, Z. -G. Li, Y. Fang, X. -Z. Wu, J. -Y. Yang, M. -G. Zhao and Y. -L. Song, *J. Mater. Chem. C.,* 2016, **4**, 4647-4653.
7. H. -Y. Liu, L. Wang, Y. -S. Wu and Q. Liao, *RSC Adv.,* 2017, **7**, 19002-19006.
8. (a) D. Chercka, S. -J. Yoo, M. Baumgarten, J. -J. Kim and K. Müllen, *J. Mater. Chem. C.,* 2014, **2**, 9083-9086. (b) Z. -J. Zhao, S. -M. Chen, J. W. Y. Lam, P. Lu, Y. -C. Zhong, K. S. Wong, H. S. Kwok and B. Z. Tang, *Chem. Commun.,* 2010, **46**, 2221-2223. (c) Y. Zhang, T. -W. Ng, F. Lu, Q. -X. Tong, S. -L. Lai, M. Y. Chan, H. -Y. Kwong and C. -S. Lee, *Dyes and Pigments.,* 2013, **98**, 190-194. (d) R. Zhang, Y. Zhao, T. -F. Zhang, L. Xu and Z. -H. Ni, *Dyes and Pigments.,* 2016, **130**, 106-115. (e) T.M. Figueira-Darte and K. Mullen, *Chem. Rev.*, 2011, **111**, 7260–7314. (e) P. Jin, T. Song, J Xiao and Q. Zhang, *Asian J. Org. Chem*., 2018, **7**, 2130 –2146.
9. (a) J. Kwon, J. -P. Hong, S. Lee and J. -I. Hong, *New J. Chem.,* 2013, **37**, 2881-2887. (b) R. -R. Fang, R. Chen, J. -H. Gao, H. -R. Zhang, H. -Z. Wu and H. -X. Li, Org. Electron. 2017, **45**, 108-114. (c) H. -J. Ju, K. Wang, J. Zhang, H. Geng, Z. -T. Liu, G. -X. Zhang, Y. -S. Zhao and D. -Q. Zhang, *Chem. Mater.,* 2017, **29**, 3580-3588. (d) P. -Y. Gu, J. Zhang, G. -K. Long, Z. -L. Wang and Q. -C. Zhang, *J. Mater. Chem. C.,* 2016, **4**, 3809-3814.
10. (a) J. -J. Shao, J. -J. Chang and C. -Y. Chi, *Org. Biomol. Chem.,* 2012, **10**, 7045-7052. (b) A. B. Marco, D. Cortizo-Lacalle, C. Gozalvez, M. Olano, A. Atxabal, X. -N. Sun, M. Melle-Franco, L. E. Hueso and A. Mateo-Alonso, *Chem. Commun.,* 2015, **51**, 10754-10757. (c) Z. -H. Wu, Z. -T. Huang, R. -X. Guo, C. -L. Sun, L. -C. Chen, B. Sun, Z. -F. Shi, X. Shao, H. Li and H. -L. Zhang, *Angew. Chem. Int. Ed.*, 2017, **56**, 13031-13035. (d) N. Kulisic, S. More and A. Mateo-Alonso, *Chem. Commun.*, 2011, **47**, 514-516. (e) P-Y. Gu, Z. Wang, G. Liu, H. Yao, Z. Wang, Y. Li, J. Zhu, S. Li and Q. Zhang, *Chem. Mater.*, 2017, **29**, 4172–4175.
11. Y. Sakamoto, T. Suzuki, M. Kobayashi, Y. Gao, Y. Fukai, Y. Inoue, F. Sato and S. Tokito, *J. Am. Chem. Soc.,* 2004, **126**, 8138-8140.
12. (a) A. Facchetti, M. Mushrush, H. E. Katz and T. J. Marks. *Adv. Mater.,* 2003, **15**, 33-38. (b) H. -J. Zhang, Y. Wang, K. -Z. Shao, Y. -Q. Liu, S. -Y. Chen, W. -F . Qiu, X. -B. Sun, T. Qi, Y. -Q. Ma, G. Yu, Z. -M. Sun and D. -B. Zhu. *Chem. Commun.,* 2006, **43**, 755-757.
13. T. M. Pappenfus, R. J. Chesterfield, C. D. Frisbie, K. R. Mann, J. Casado, J. D. Raff and L. L. Miller, *J. Am. Chem. Soc.,* 2002, **124**, 4184-4185.
14. (a) R. Furue, T. Nishimoto, I. S. Park, J. Lee and T. Yasuda, *Angew. Chem. Int. Ed.,* 2016, **55**, 7171-7175. (b) G. -Z. Xie, D. -J. Chen, X. -L. Li, X. -Y. Cai, Y. -C. Li, D. -C. Chen, K. -K. Liu, Q. Zhang, Y. Cao and S. -J. Su, *ACS Appl. Mater. Interfaces.,* 2016, **8**, 27920-27930.
15. (a) H. Muraoka, T. Obara and S. Ogawa, *Tetrahedron Lett.,* 2016, **57**, 3011-3015. (b) P. Wei, Z. -X. Gao, R. Zhang, A. Li, F. Zhang, J. Li, J. -J. Xie, Y. -Z. Wu, M. Wu and K. -P. Guo, *J. Mater. Chem. C.,* 2017, **5**, 6136-6143. (c) V. Palakollu and S. Kanvah, *New J. Chem.,* 2014, **38**, 5736-5746.
16. (a) A. Facchetti, M. -H. Yoon, C. L. Stern, G. R. Hutchison, M. A. Ratner and T. J. Marks, *J. Am. Chem. Soc.,* 2004, **126**, 13480-13501. (b) F. Babudri, G. M. Farinola, F. Naso and R. Ragni, *Chem. Commun*., 2007, **44**, 1003-1022.
17. T. H. El-Assad, M. Auer, R. Castaneda, K. M. Hallal, F. M. Jradi, L. Mosca, R. S. Khnayzer, D. Patra, T. V. Timofeeva, J-L. Bredas, E. J. W. List-Kratochvil, B. Wax, B. R. Kaafarani; *J.Mater.Chem.C.*, 2016, **4**, 3041-3058.
18. M. J.Turner, J. J. McKinnon, S. K. Wolff, D. J. Grimwood, P. R. Spackman, D. Jayatilaka, M. A. Spackman, CrystalExplorer (Version 17.5), University of

Western Australia, 2018.
19. Y. -L. Qiao, J. Zhang, W. Xu and D. -B. Zhu, *Tetrahedron.,* 2011, **67**, 3395-3405.
20. A. Kathiravan, V. Srinivasan, T. Khamrang, M. Velusamy, M. Jaccob, N. Pavithra, S. Anadan and K. Velappan, *Phys. Chem. Chem. Phys.,* 2017, **19**, 3125-3135.
21. M. Ashizawa, K. Yamada, A. Fukaya, R. Kato, K. Hara and J. Takeya, *Chem. Mater.,* 2008, **20**, 4483-4890.
22. X. Y. Shen, Y. J. Wang, E. Zhao, W. Z. Yuan, Y. Liu, P. Lu, A. Qin, Y. -G. Ma, J. Z. Sun and B. Z. Tang, *J. Phys. Chem. C.,* 2013, **117**, 7334-7337.
23. N. Deshapande, N. S. Belavagi, M. G. Sunagar, S. Gaonkar, G. H. Pujar, M. N. Wari, S. R. Inamdar and I. A. M. Khazi, *Rsc Adv.,* 2015, **5**, 86685-86696.
24. X. Feng, J. -Y. Hu, H. Tomiyusa, N. Seto, C. Redshaw, M. R. J. Elsegood and T. Yamato, *Org. Biomol. Chem.,* 2013, **11**, 8366-8374.
25. (a) X. J. Gong, Y. P. Pan, X. Xie, T. Tong, R. F. Chen and D. Q. Gao, *Opt. Mater.* 2018, **78**, 94-101.(b) M. L. Liu, X. J. Gong, C. Y. Zheng and D. Q. Gao, *Asian J. Org. Chem.* 2017, **6**, 1903-1913.
26. M. Beinhoff, W. Weigel, M. Jurczok, W. Rettig, C. Modrakowski, I. Brüdgam, H. Hartl and A. D. Schlüter, *Eur J. Org. Chem.* 2001, 3819-3829.
27. O. V. Dolomanov, L. J. Bourhis, R. J. Gildea, J. A. K. Howard and H. Puschmann, *J. Appl. Cryst.* 2009, **42**, 339-341.
28. G.M. Sheldrick, *Acta Cryst.* 2008, **A64**, 112-122.

Entry for the Table of Contents

Insert graphic for Table of Contents here.

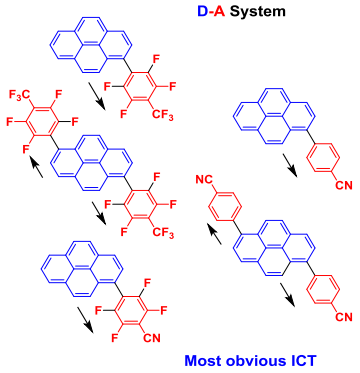

In pyrene Donor-Acceptor systems, the cyano groups extend the conjugated π system while fluoroaryl groups induce intramolecular charge transfer (ICT). Due to synergy of conjugation and ICT, the mono-aryl pyrenes have stronger solvatochromism than the di-aryl systems and fluoroaryl pyrenes have stronger solvatochromism than nonfluorinated analogues. The perfluorotolyl-pyrene has close stacking (3.44 Á.between planes) and forms anti-parallel dimers due to short CH...F contact and the distance between